

Characterisation of a laboratory electrochemical ozonation system and its application in advanced oxidation processes

LEONARDO M. DA SILVA¹, DÉBORA V. FRANCO², JULIANE C. FORTI³, WILSON F. JARDIM¹
and JULIEN F.C. BOODTS^{2,*}

¹*Instituto de Química, Universidade Estadual de Campinas, Cidade Universitária Zeferino Vaz, 13083-970, Campinas, SP, Brazil*

²*Instituto de Química, Universidade Federal de Uberlândia, Campus Santa Mônica, Av. João Naves de Ávila 2160, 38400-902, Uberlândia, MG, Brazil*

³*Departamento de Química, Faculdade de Filosofia Ciências e Letras de Ribeirão Preto, Universidade de São Paulo, Av. Bandeirantes 3900, 14040-901, Ribeirão Preto, SP, Brazil*

(*author for correspondence, tel.: +55-34-32394143, fax: +55-34-32394208, E-mail: jfcboodts@ufu.br)

Received 4 April 2005; accepted in revised form 2 September 2005

Key words: advanced oxidation processes, degradation, Electrochemistry, ozone, reactive dyes

Abstract

An electrochemical reactor for oxygen/ozone production was developed using perforated planar electrodes. An electroformed β -PbO₂ coating, deposited on a platinised titanium substrate, was employed as anode while the cathode was a platinised titanium substrate. The electrodes were pressed against a solid polymer electrolyte to minimise ohmic drop and avoid mixing of the gaseous products (H₂ and O₂/O₃). Electrochemical ozone production (EOP) was investigated as function of current density, temperature and electrolyte composition. Electrochemical characterisation demonstrated ozone current efficiency, Φ_{EOP} , ozone production rate (g h⁻¹), v_{EOP} , and grams of O₃ per total energy demand (g h⁻¹ W⁻¹), v_{EOP} increase on decreasing electrolyte temperature and increasing current density. The best reactor performance for EOP was obtained with the base electrolyte (H₂SO₄ 3.0 mol dm⁻³) containing 0.03 mol dm⁻³ KPF₆. Degradation of reactive dyes used in the textile industry (Reactive Yellow 143 and Reactive Blue 264) with electrochemically-generated ozone was investigated in alkaline medium as function of ozone load (mg h⁻¹) and ozonation time. This investigation revealed ozonation presents very good efficiency for both solution decolouration and total organic carbon (TOC) removal.

1. Introduction

Oxidation of organic pollutants (e.g. dyes of the textile industry, pesticides, etc.) can be carried out using appropriate anodically formed oxidants, as in the case of ozone [1–5]. The so-called Advanced Oxidation Processes (AOP) allows the optimisation of ozone application by increasing the concentration of hydroxyl radicals (HO· – $E^0 = 2.80$ V) resulting from O₃-decomposition in aqueous solutions, permitting a significant increase in decomposition rate for recalcitrant pollutants [1, 3, 5–7].

Different ozonation systems based on electrochemical technology have been described [6, 8–11]. Electrochemical reactors for ozone production can be constructed making use of a solid polymer electrolyte and high-porosity 3D-electrodes [6, 8–10]. In this configuration ozone is released directly in the electrolyte-free water stream. Such technology gives a high O₃-concentration

in the gaseous phase (~14 wt. %), and presents high gas dispersion into the aqueous phase. Ozone can also be generated in another reactor configuration using hollow cylindrical fluorocarbon-impregnated carbon anodes and solid polymer electrolyte technology [1]. Inherent advantages of this ozonation system are its high current efficiencies (~35%), lower cell voltage and elimination of hydrogen management through the use of air cathodes [6, 12]. The disadvantage of this configuration is that decomposition of organics is limited by the ozone mass transfer rate from the gas to the liquid phase, where it is needed for reaction with organics.

Ozonation systems based on electrochemical technology are a promising alternative to the conventional ozonation systems (corona process) especially in the case where high O₃-concentrations are required (e.g. decomposition of resistant organic pollutants such as dyes and pesticides).

This paper reports the characterisation of an electrochemical ozonation system based on the use of perforated planar electrodes and its application to the degradation of some reactive dyes used in the textile industry with electrochemically generated ozone.

2. Experimental details

2.1. Electrochemical reactor

The reactor consisted of symmetric perforated planar electrodes ($10 \times 8 \times 0.15$ cm) pressed against a solid polymer electrolyte, SPE, (Nafion® 117). The geometric area of the perforated electrodes was 137 cm^2 , while the electrode area in intimate contact with the solution was 80 cm^2 . Electrodes were perforated to avoid blockage of the electric field and permit proton transport between cathode and anode. The $\beta\text{-PbO}_2$ electrode was prepared by electrodeposition at constant current from acid $\text{Pb}(\text{NO}_3)_2$ solution onto both faces of a steel micro-sphere blasted perforated Ti-support, previously etched for 10 min in boiling oxalic acid (10% w/w) and then platinised. Pt electrodeposition was carried out at constant current density (30 mA cm^{-2}) for 20 min from a solution containing $10 \text{ g dm}^{-3} \text{H}_2\text{PtCl}_6 + 10 \text{ mg dm}^{-3} \text{Pb}(\text{CH}_3\text{CO}_2)_2 \cdot 3\text{H}_2\text{O}$, at $24 \text{ }^\circ\text{C}$. $\beta\text{-PbO}_2$ was electrodeposited at constant current density of 30 mA cm^{-2} for 1 h onto both sides of the platinised Ti-support from a solution containing $0.01 \text{ mol dm}^{-3} \text{HNO}_3 + 0.2 \text{ mol dm}^{-3} \text{Pb}(\text{NO}_3)_2$, at $60 \text{ }^\circ\text{C}$. The average thickness of the $\beta\text{-PbO}_2$ layer, estimated by weighing, was approximately $40 \text{ }\mu\text{m}$. Fluka "purum" products were used throughout.

The cathode consisted of a perforated platinised titanium substrate prepared under identical conditions as described above using an electrodeposition time of 1 h. Nafion® 117 SPE was pre-treated in boiling nitric acid (50%) for 30 min and hydrated in boiling deionised water for 2 h [13].

Figure 1 shows a scheme of the reactor while Figure 2 presents the experimental set-up used in the investigation. The reactor compartments were manufactured from 1-inch thick acryl plates, while Viton® tubes were employed to circulate the electrolyte between the anodic reactor compartment and the all-glass electrolyte reservoir/gas separator flask (5 dm^3). The anodically formed gases ($\text{O}_2 + \text{O}_3$) were separated from the electrolyte in the gas separator flask and transported to the spectrophotometer using N_2 as carrier gas. In the dye degradation investigation the O_2/O_3 mixture was passed directly into the Reactor Flask containing the reactive dye.

2.2. Equipment and techniques

Ozone concentration in the gaseous phase was analysed by UV absorption measurements at 254 nm , using a homemade gas flow cell. Absorbance was read after 15 min of cell polarisation when steady state conditions were observed. EOP partial current, j_{EOP} , and EOP current efficiency, Φ_{EOP} , were calculated using the equations [2, 14]:

$$j_{\text{EOP}} = (A \overset{\circ}{V} zF) / (\varepsilon l) \quad (1)$$

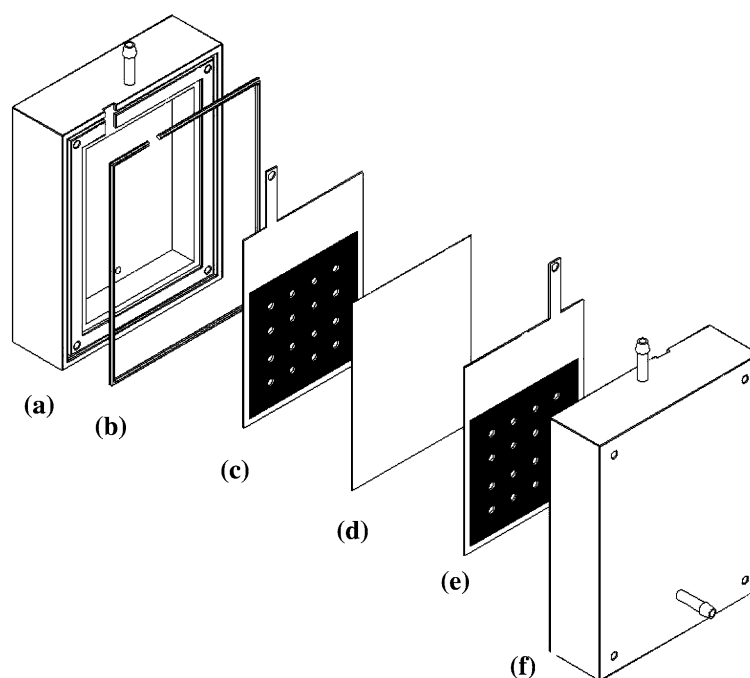


Fig. 1. Scheme of the electrochemical reactor for ozone production. (a) cathodic compartment; (b) rubber gasket (Viton®); (c) cathode, Ti^0/Pt^0 ; (d) SPE, Nafion® 117; (e) anode, $\text{Ti}/\text{Pt}/\beta\text{-PbO}_2$; (f) anodic compartment.

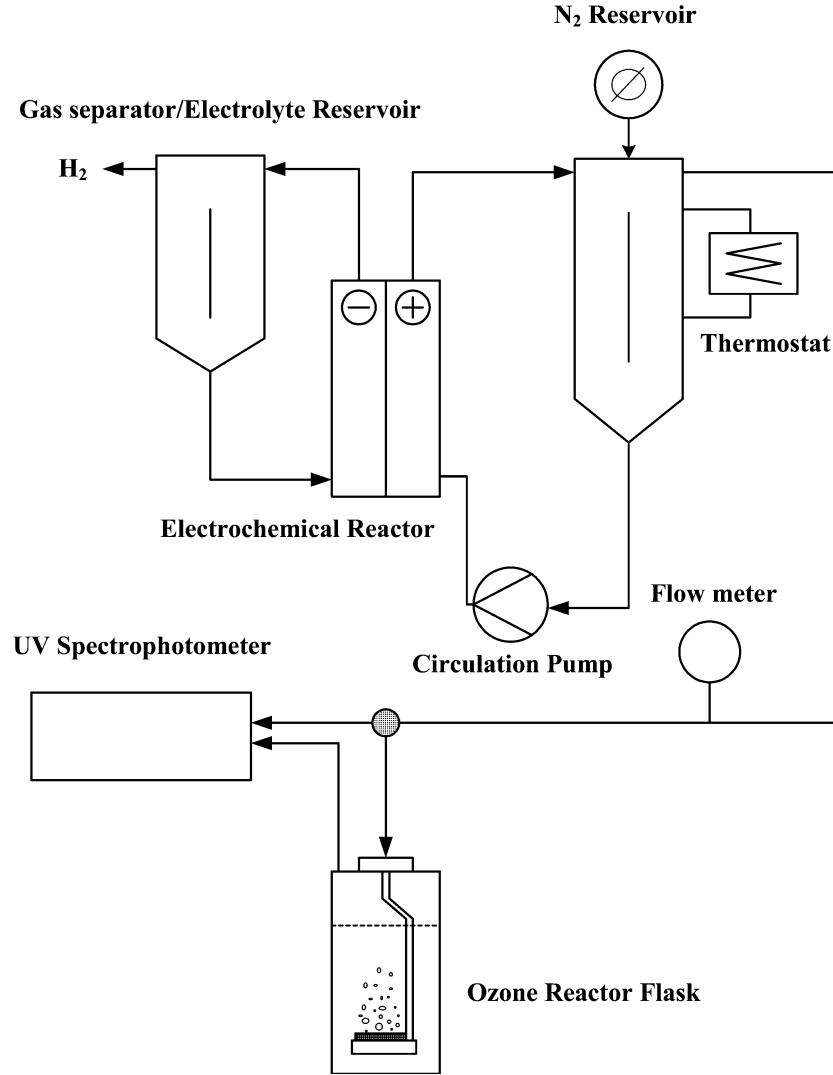


Fig. 2. Experimental set up employed for ozone generation and investigation of decolouration/degradation of textile dyes.

$$\Phi_{\text{EOP}}(\%) = [(A \dot{V} z F) / (\varepsilon l I_T)] 100 \quad (2)$$

where: A = absorbance at 254 nm; \dot{V} = volumetric flow rate of ($\text{N}_2 + \text{O}_2 + \text{O}_3$) ($\text{dm}^3 \text{ s}^{-1}$); z = number of electrons ($z=6$); ε = ozone absorptivity at 254 nm ($3024 \text{ cm}^{-1} \text{ mol}^{-1} \text{ dm}^3$ [15]); l = optical path length (0.63 cm); I_T = total current (OER + EOP) (ampère); F = Faraday's constant (96485 C mol^{-1}). The EOP specific power consumption, P_{EOP}^0 , was calculated using the equation [16]:

$$P_{\text{EOP}}^0 (\text{Wh g}^{-1}) = (U z F) / (1.73 \times 10^5 \Phi_{\text{EOP}}) \quad (3)$$

where U is the cell voltage.

The reactor performance for the EOP was investigated as functions of the operating parameters analysing the “ozone production rate”, v_{EOP} , and the parameter “gain of ozone mass per total power consumption”, ϑ_{EOP} , which were calculated according to Equations 4 and 5, respectively [16]:

$$v_{\text{EOP}} (\text{g h}^{-1}) = 3600 (j_{\text{EOP}} M) / (z F) \quad (4)$$

$$\vartheta_{\text{EOP}} (\text{g W}^{-1} \text{h}^{-1}) = v_{\text{EOP}} / I_T U \quad (5)$$

where M is the ozone molecular weight (48 g mol^{-1}).

The electrochemical reactor was powered by a 80 A/12 V d.c. current source. The electrolytes used consisted of sulphuric acid solutions, in the presence or absence of fluor-compounds. In all cases the electrolyte was circulated in the anodic compartment using a model 7018-21 MASTERFLEX peristaltic circulation pump (Cole-Parmer). The linear velocity of the electrolyte was 1.30 cm s^{-1} and the space velocity 5.19 min^{-1} . The flow regime was turbulent ($\text{Re} > 3000$). Temperature control was achieved by means of a model FC55A01 FTS cooling system connected to the all-glass electrolyte reservoir/gas separator flask. The electrolyte temperature at the anode surface was monitored using a model 61 FLUKE digital thermocouple.

2.3. Ozonation of aqueous textile dye solutions

The decolouration/degradation efficiency of the ozonation process was evaluated using as model recalcitrant compounds reactive dyes employed in the textile industry. The decolouration/degradation of C.I. Reactive Yellow 143 (RY 143) and C.I. Reactive Blue 264 (RB 264) dyes were carried out in alkaline solutions (pH = 10) containing 150 ppm of these compounds. The samples were prepared by dissolving the commercial dyes, furnished by CERMATEX Textile Industry Ltd. (Americana, Brazil), in distilled water.

Decolouration of 40 ml samples of reactive dyes was followed spectrophotometrically measuring the absorbance at their maximum wavelength of absorbance (421 and 619 nm for RY 143 and RB 264, respectively) as functions of the ozonation time. A model D4000 HACH Spectrophotometer was used throughout. Removal of the total organic carbon (TOC) was investigated by measuring the TOC-decay as a function of ozonation time. TOC measurements were carried out using a model 2000 Shimadzu TOC Analyser.

Gas dispersion in the reactor flask was done passing the gas mixture ($O_2 + O_3$) through a gas diffuser (Shott #2 coarse glass frit) placed at the bottom of the ozone reactor flask. Non-reacted ozone at the flask outlet was analysed spectrophotometrically at 254 nm as a function of ozonation time. Figure 2 shows the set up used for ozone generation and degradation of the textile dyes.

3. Results and discussion

3.1. Characterisation of the electrochemical ozonation system

Previous studies [2, 14] showed galvanostatic polarisation of β -PbO₂ electrodes produces a transient behaviour of the electrode potential and EOP-current efficiency. Therefore, the galvanostatic polarization experiments were carried out by recording the cell voltage, U , and measuring ozone absorbance after 15 min of polarisation when a steady response was observed. Figure 3 shows the dependence of U and Φ_{EOP} on I_T , for different temperatures.

Figure 3a shows that U -values are little affected by temperature for $I_T \leq 30$ A; however, for higher I_T -values a reduction in temperature is accompanied by an increase in the cell overvoltage. Figure 3b and c show the dependence of Φ_{EOP} on I_T and temperature for the 1.0 and 3.0 mol dm⁻³ H₂SO₄ electrolytes, respectively. Φ_{EOP} increases on increasing I_T and decreasing temperature, giving values in the ~0.5–4% current efficiency interval. In agreement with the fundamental studies presented by Foller and Tobias [17], Φ_{EOP} -values increase with increasing sulphuric acid concentration. This behaviour differs from the set-up using high-porosity 3D-electrodes (lead dioxide supported on

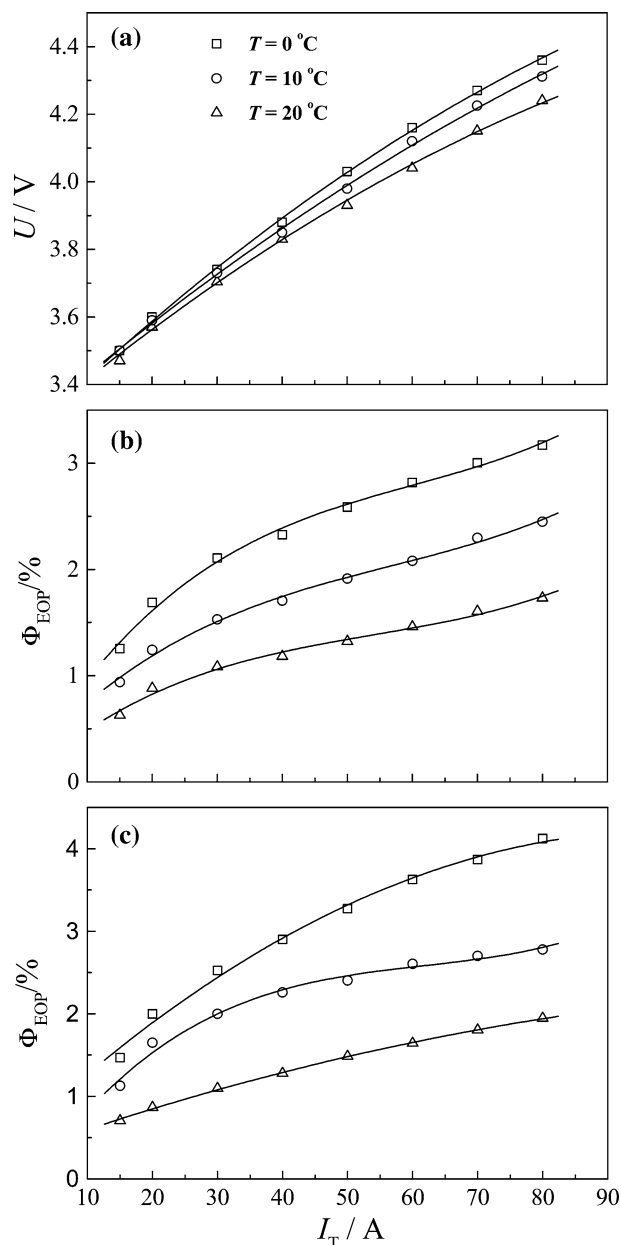


Fig. 3. Dependence of cell voltage, U , and EOP current efficiency, Φ_{EOP} , on total current, I_T , and temperature. Electrolyte: (a) and (b) 1.0 mol dm⁻³ H₂SO₄; (c) 3.0 mol dm⁻³ H₂SO₄.

porous titanium substrate), where a maximum in Φ_{EOP} is reached at moderate temperatures (~30 °C) [8, 9].

Due to the rather different surface current distribution and bubble adherence at the electrode surface, comparison of the behaviour of perforated planar electrodes and high-porosity 3D-electrodes is very difficult [8, 9, 18, 19]. While with planar electrodes in contact with conventional electrolytes all regions of the electrode surface are, in principle active, in the case of high-porosity 3D-electrodes making use of electrolyte-free water the active surface area is restricted to the electrode regions in intimate contact with the solid polymer electrolyte [18, 19].

Figure 4 shows the dependency of the EOP specific power consumption, P_{EOP}^0 , ozone production rate, v_{EOP} ,

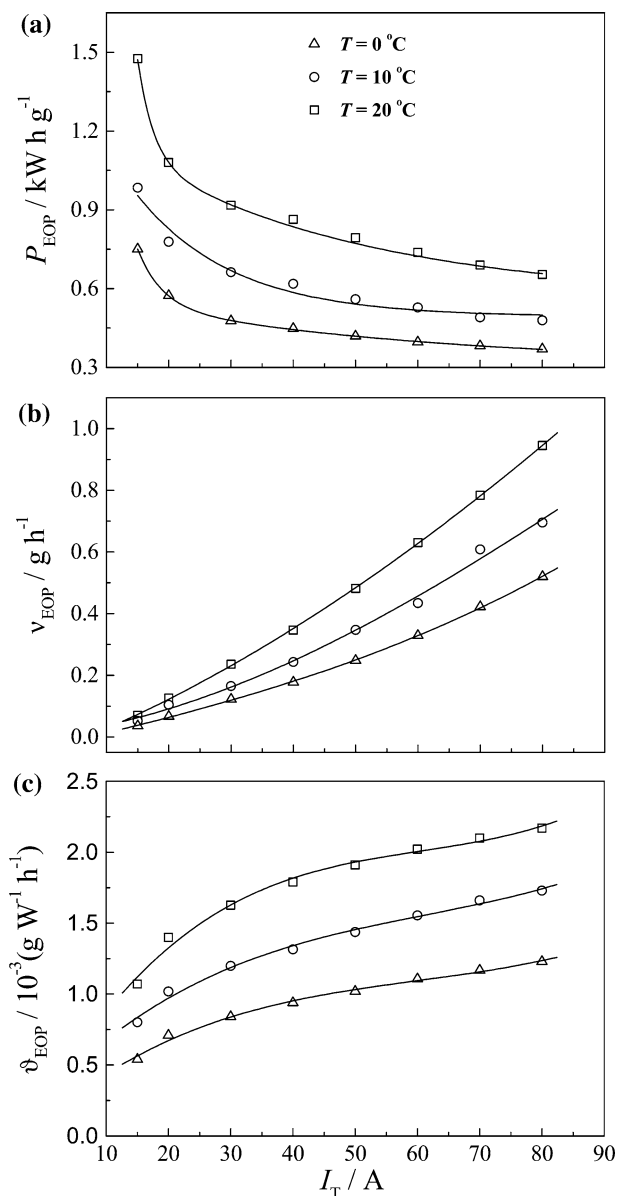


Fig. 4. Dependence of EOP specific power consumption, P_{EOP}^0 , ozone production rate, v_{EOP} , and gain of ozone mass per total power consumption, ϑ_{EOP} , on total applied current, I_T , and electrolyte temperature. Electrolyte: $3.0 \text{ mol dm}^{-3} \text{ H}_2\text{SO}_4$.

and the gain of ozone mass per total power consumption, ϑ_{EOP} , on I_T and temperature for the $3.0 \text{ mol dm}^{-3} \text{ H}_2\text{SO}_4$ electrolyte.

P_{EOP}^0 -values decrease with increasing I_T and decreasing temperature, giving values in the $1.5\text{--}0.4 \text{ kW h g}^{-1}$ interval (Figure 4a). Comparison with the literature [8–10] shows these values are higher for perforated planar electrodes. Figure 4b and c show that both v_{EOP} and ϑ_{EOP} are affected by temperature and current density. Maximum ozone production occurs at high current densities, where minimum power consumption is observed. Figure 4c also shows that the best EOP performance (maximum ϑ_{EOP} -value) is reached at high I_T -values and low temperatures.

Several studies [2, 5, 12, 17] have shown that the introduction of additives (e.g. NaF, HBF₄, KPF₆) to the

base electrolyte (e.g. H₂SO₄) significantly increases EOP current efficiency. Foller and Kelsall [12] reported EOP current efficiencies of up to 45% with an electrochemical reactor using tubular glassy carbon as anode and concentrated fluorboric acid (62 wt. %) as electrolyte. Fundamental aspects of the influence of the electrolyte and electrode material on the EOP process were discussed previously [2, 14, 16].

Figure 5 shows the influence, for several temperatures, of the introduction of KPF₆ to the electrolyte ($3.0 \text{ mol dm}^{-3} \text{ H}_2\text{SO}_4$) on the current efficiency and specific power consumption for the EOP process.

Comparing Figures 3 and 5 it is observed that introduction of KPF₆ considerably increases Φ_{EOP} . As discussed by Foller and Kelsall [12], EOP current efficiencies higher than 20%, obtained at high current densities, imply a specific generation rate per unit electrode area of up to three times that of corona discharge technology. Figure 5b shows that the EOP energy demand decreases at high I_T -values and low temperature, reaching a minimum of 60 Wh g^{-1} at $0^\circ C$ for $I_T > 40 \text{ A}$. This result is identical to that reported for high-porosity 3D-electrodes [8–10].

Ozone production rate, v_{EOP} , and gain of ozone mass per total power consumption, ϑ_{EOP} , calculated for the electrolyte containing $0.03 \text{ mol dm}^{-3} \text{ KPF}_6$ as functions of I_T and temperature are presented in Figure 6.

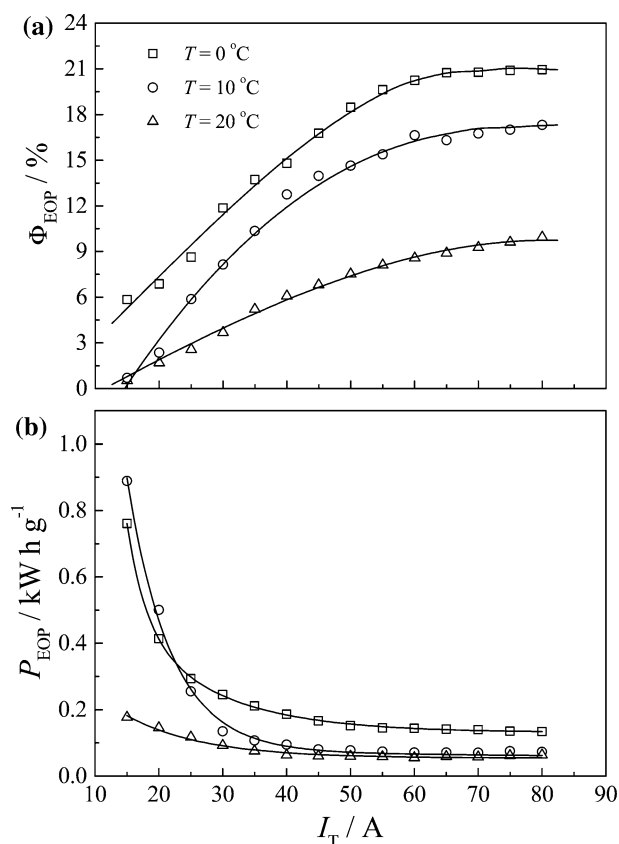


Fig. 5. Dependence of EOP current efficiency, Φ_{EOP} , and EOP specific power consumption, P_{EOP}^0 , on total applied current, I_T , and electrolyte temperature. Electrolyte: $3.0 \text{ mol dm}^{-3} \text{ H}_2\text{SO}_4 + 0.03 \text{ mol dm}^{-3} \text{ KPF}_6$.

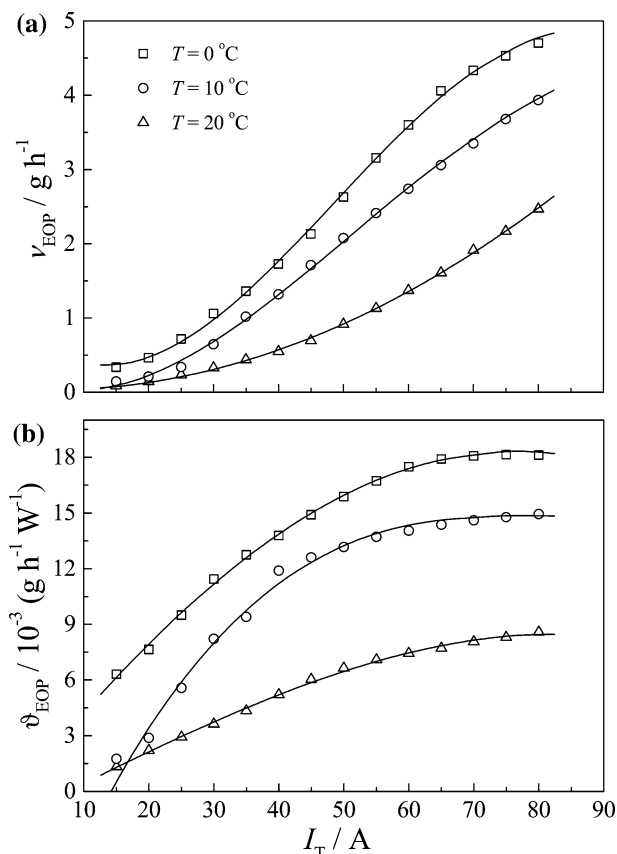


Fig. 6. Dependence of ozone production rate, v_{EOP} , and gain of ozone mass per total power consumption, ϑ_{EOP} , on total applied current, I_T , and electrolyte temperature. Electrolyte: $3.0 \text{ mol dm}^{-3} \text{ H}_2\text{SO}_4 + 0.03 \text{ mol dm}^{-3} \text{ KPF}_6$.

Comparison of Figures 4b and 6a shows that ozone production rates increase significantly when KPF_6 is added to the sulphuric acid electrolyte. The maximum ozone production rate of 4.7 g h^{-1} is higher than the corresponding rate reported for high-porosity 3D-electrodes ($\sim 0.8 \text{ g h}^{-1}$) [8], and comparable to the rate in reactors using tubular glassy carbon anodes (5 g h^{-1}) [12]. Figure 6b shows that introduction of KPF_6 promotes a significant increase in the gain of ozone mass per total power consumption, thus showing a substantial reduction in the energy demand.

3.2. Decomposition of reactive dyes with electrochemically generated ozone

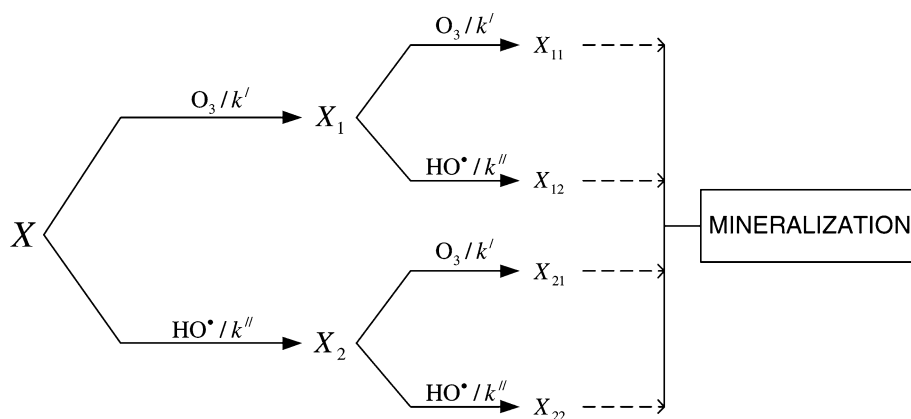
Ozonation kinetics of textile dye solutions depends on solution pH, initial dye concentration (IDC) and ozone load [20, 21]. While the influence of IDC and ozone load is straightforward, the influence of pH can be understood considering that when ozone is solubilized in water, hydroxide ions (HO^-) initiate a chain reaction leading to ozone degradation generating several oxygenated radicals among them the hydroxyl radical (HO^\bullet) [22]. The hydroxyl radical (HO^\bullet), the basis of the so-called advanced oxidation processes (AOP), is the most important specie formed due to its non-selectivity and much higher redox potential ($E^0 = 2.80 \text{ V}$) than ozone ($E^0 = 2.07 \text{ V}$) [23].

Therefore, depending on solution pH, the overall oxidative decolouration process can be controlled either by molecular ozone (direct process) or hydroxyl radicals (indirect process), or a combination of both [21]. A scheme for the ozonation of a given parent dye molecule, X , was recently proposed by Da Silva and Jardim [24]:

According to the scheme, the extent of the ozonation reaction and the competition between both direct and indirect oxidative processes control the degree of mineralization of the parent dye molecule, thus governing the decolouration of dye solutions and the nature of persistent by-products, denoted by X_n .

It is worth emphasising that there is a distinction between decolouration of the dye solution and total degradation (mineralization). For most textile dyes, decolouration *via* chemical oxidation (e.g. ozonation) occurs when the chromophore bond is removed, while the major daughter products of the parent dye molecule may remain intact [25]. Therefore, decolouration may be the first step in the degradation route of a dye molecule, which is not necessarily accompanied by TOC removal. Thus, decolouration usually requires a lower oxidant load than mineralization.

Based on the above discussion, degradation of the reactive dyes (RY 143 and RB 264) was carried out in alkaline medium in order to favour the indirect



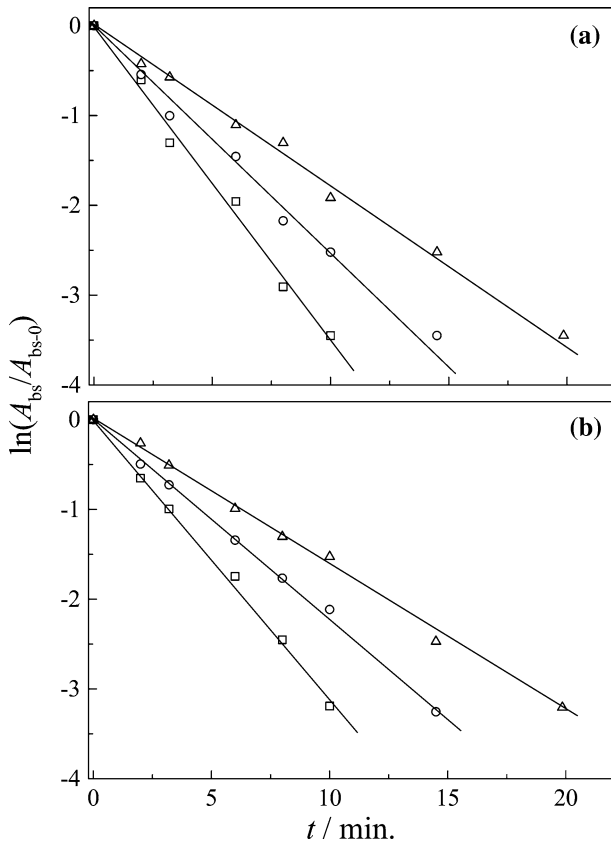


Fig. 7. Pseudo first-order behaviour representative of the decolouration kinetics. Textile dye: (a) Reactive Yellow 143 (150 ppm); (b) Reactive Blue 264 (150 ppm). pH = 10. Ozone load (mg h^{-1}): (□) 330; (○) 250; (Δ) 210. $T = 24$ °C.

oxidative route *via* HO[•] formation. The efficiency of the degradation process was investigated by monitoring the decolouration kinetics and the removal rate of total organic carbon, TOC, as functions of ozone concentration and ozonation time.

Figure 7 shows the pseudo first-order decolouration kinetics observed for the dyes RY 143 and RB 264 as a function of the ozone concentration.

Decolouration kinetics depend on ozone concentration and the chemical nature of the dye. For both RY 143 and RB 264 the pseudo-first order rate constant, k_{obs} , increases with increasing O₃-concentration, albeit, it increases with increasing HO[•]-concentration. Considering that the effluent pH in the textile industry is frequently high (>9) [25], ozone concentration is an important parameter, which should be optimised to furnish an optimum hydroxyl radical concentration in solution in order to obtain adequate effluent decolouration, before completing the treatment with the cheaper conventional biological treatment.

Decolouration efficiencies higher than 99% were obtained in all cases. The half-life time constant, $\tau_{1/2}$, decreases from 3.85 to 1.98 min (RB 264) and 4.20 to 2.22 min (RY 143), when the ozone load is increased from 210 to 330 mg h^{-1} .

Figure 8 shows the influence of ozonation time and ozone load on total organic carbon removal.

Figure 8 shows that the TOC/TOC₀-ratio decreases with increasing ozone concentration and ozonation time. These results suggest that contact time and ozone concentration are very important variables for TOC-removal. A strong decrease in the TOC/TOC₀-ratio is observed for short ozonation times while for longer times the ratio levels off.

Analysis of these findings also reveals that TOC/TOC₀ decay does not have pseudo first-order kinetics. This behaviour indicates that degradation takes place *via* direct (ozone) and indirect (hydroxyl radical) oxidation processes, where the overall oxidative route is mainly characterised by a low oxidant concentration. As a consequence, only partial mineralization is achieved and a considerable amount of persistent by-products is formed. Indeed, TOC-removal values after 60 min of ozonation were 40, 45 and 55% (RY 143) and 33, 37 and 46% (RB 264), for O₃-concentrations of 210, 250 and 330 mg h^{-1} , respectively.

Comparison of these experimental data (see Figures 7 and 8) with literature reports for different AOP [26], suggests that ozonation in alkaline medium is a very efficient process for both decolouration and TOC-removal, despite the later being less pronounced. These results are consistent with the fact that, after the primary attack of the dye's molecular structure (conjugated system), which is mainly responsible for decolouration

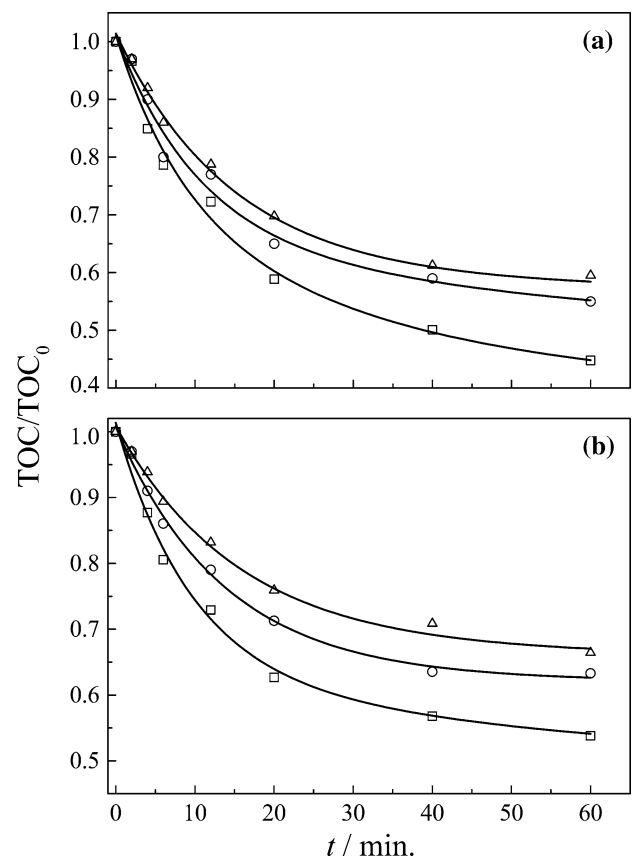


Fig. 8. Influence of ozonation time and ozone concentration on the reduction of total organic carbon, TOC. Textile dye: (a) Reactive Yellow 143 (150 ppm); (b) Reactive Blue 264 (150 ppm). pH = 10. Ozone load (mg h^{-1}): (□) 330; (○) 250; (Δ) 210. $T = 24$ °C.

[27], the resulting parent fragments having lower or non chromophore activity are further degraded by the hydroxyl radicals supplied to the solution *via* continuous ozonation. Thus, after the initial rapid decolouration of the solution (breakdown of the conjugated system of the dye), degradation is sustained by a continuous attack by the hydroxyl radical of fragments possessing a higher recalcitrant nature.

The ozonation process is very sensitive to the nature of the gas dispersion system that controls the mass transfer rate of the gas into the liquid phase [28, 29]. Thus, in applications involving treatment of residuary waters/effluents containing recalcitrant organics the gas dispersion system should be optimised together with the ozone concentration in order to increase the degradation kinetics and reduce ozone loss. When an efficient gas dispersion system is employed under dynamic conditions the unreacted ozone leaving the residuary water can be significantly reduced, presenting O₃-capture efficiencies higher than 90% [28].

The results presented clearly show that electrochemical ozone production is an attractive technology for water/effluent treatment. The development and optimisation of electrolytic ozonation systems, allied with the optimisation of important parameters, such as (i) ozone concentration; (ii) effluent pH; (iii) gas dispersion system and (iv) TOC-removal, constitute an important issue in environmentally friendly technologies oriented towards effluent treatment.

4. Conclusions

Characterisation of an electrochemical ozonation system showed that ozone production depends on current density, chemical composition and electrolyte temperature. Ozone current efficiency values in the 0.5–21% interval were obtained as functions of these parameters. This wide range of current efficiency permits high flexibility for its application. Maximum ozone production was obtained at high current densities and low temperature for sulphuric acid solution (3.0 mol dm⁻³) containing the KPF₆ (0.03 mol dm⁻³). Analysis of the energy demand, based on the determination of the gain in ozone mass per total power consumption, revealed that optimising operational parameters could reduce the cost associated with electrochemical ozone production.

Decolouration/degradation of reactive dyes employed in the textile industry (RY 143 and RB 264) was carried out, and revealed that ozonation is very efficient for both decolouration and removal of total organic carbon. However, due to the higher cost of electrochemically generated ozone, total organic carbon removal should be conducted to such an extent that cheaper treatments (e.g. biological) complete the degradation process. The results obtained strongly support further

development and optimisation of electrochemical technology for ozone production.

Acknowledgements

L.M. Da Silva, J.C.Fórti and W.F. Jardim acknowledge the FAPESP Foundation. D.V. Franco and J.F.C. Boodts thank the FAPEMIG Foundation. The authors also thank Dr. C. Collins.

References

1. H. Jüttner, U. Galla and H. Schmieder, *Electrochim. Acta* **45** (2000) 2575.
2. L.M. Da Silva, L.A. De Faria and J.F.C. Boodts, *Pure Appl. Chem.* **73** (2001) 1871.
3. L.M. Da Silva, M.H.P. Santana and J.F.C. Boodts, *Quim. Nova* **26** (2003) 880.
4. F.C. Walsh, *Pure Appl. Chem.* **73** (2001) 1819.
5. R.G. Rice and A. Netzer, *Handbook of Ozone Technology and Applications 1* (Ann Arbor Science, New York, 1982).
6. P. Tatapudi and J.M. Fenton, in C.A.C. Sequeira (Ed), *Environmental Oriented Electrochemistry*, (Elsevier, Amsterdam, The Netherlands, 1994), pp. 103.
7. E.K. Winarno and N. Getoff, *Radiat. Phys. Chem.* **65** (2002) 387.
8. S. Stucki, G. Theis, R. Kötzt, H. Devantay and H.J. Christen, *J. Electrochem. Soc.* **132** (1985) 367.
9. S. Stucki, H. Baumann, H.J. Christen and R. Kötzt, *J. Appl. Electrochem.* **17** (1987) 773.
10. Y. Zhou, B. Wu, R. Gao, H. Zhang and W. Jiang, *Yingyoung Huaxue* **13** (1996) 95.
11. J.E. Graves, D. Pletcher, R.L. Clarke and F.C. Walsh, *J. Appl. Electrochem.* **22** (1992) 200.
12. P.C. Foller and G.H. Kelsall, *J. Appl. Electrochem.* **23** (1993) 996.
13. O. Simond and Ch. Comninellis, *Electrochim. Acta* **42** (1997) 2013.
14. L.M. Da Silva, L.A. de Faria and J.F.C. Boodts, *Electrochim. Acta* **48** (2003) 699.
15. O. Leitzke, Internationales Symposium Ozon und Wasser, Berlin, Germany, 14–17 September (1977) pp. 164–166.
16. L.M. Da Silva, Investigation of the Electrochemical Technology for Ozone Production: Fundamentals and Applied Aspects, Thesis, Chemistry Department/FFCLRP, University of São Paulo, Ribeirão Preto (2004).
17. P.C. Foller and C.W. Tobias, *J. Electrochem. Soc.* **129** (1982) 505.
18. P.J. Gellings and H.J.M. Bouwmeester, *The CRC Handbook of Solid State Electrochemistry* (CRC Press, Enschede, The Netherlands, 1996).
19. K. Scott, *Electrochemical Processes for Clean Technology* (The Royal Society of Chemistry, Cambridge, UK, 1995).
20. H. Selcuk, *Dyes Pigments* **64** (2005) 217.
21. W. Chu and C.W. Ma, *Wat. Res.* **34** (2000) 3153.
22. F.W. Pontius, *Water Quality and Treatment* (American Water Works Association, McGraw-Hill, New York, 1990).
23. N. Zoubov and M. Pourbaix, in M. Pourbaix (Ed), *Atlas of Electrochemical Equilibria in Aqueous Solutions*, (NACE International, Texas, 1974), pp. 540.
24. L.M. Da Silva and W.F. Jardim, *Quim. Nova*, in press.
25. O.J. Hao, H. Kim and Chiang Pen-Chi, *Crit. Rev. Environm. Sci. Technol.* **30** (2000) 449.
26. E. Kusvuran, O. Gulnaz, S. Irmak, O.M. Atanur, H.I. Yavuz and O. Erbatur, *J. Hazardous Mater.* **B109** (2004) 85.
27. N.H. Ince and G. Tezcanlı, *Dyes Pigments* **49** (2001) 145.
28. Y.C. Hsu, J.T. Chen, H.C. Yang and J.H. Chen, *AIChE J.* **47** (2001) 169.
29. S.H. Lin and C.H. Wang, *J. Hazardous Mater.* **B98** (2003) 295.